Molecules at early epochs. VI - A search for the molecular hydrogen in the Z = 3.391 damped Lyman alpha system toward Q0000-263

Levshakov, S.A.; Chaffee, F.H.; Foltz, C.B.; Black, J.H.

Astron. Astrophys. 262, 385–394 (1992)

ASTRONOMY AND ASTROPHYSICS

Molecules at early epochs*

VI. A search for molecular hydrogen in the $z = 3.391$ damped Lyman alpha system toward Q0000-263

S.A. Levshakov[1] ** **F.H. Chaffee[2]** *** **C.B. Foltz[2]** **and J.H. Black[3]** ****

[1] A.F. Ioffe Physico-Technical Institute, St. Petersburg 194021, Russia
[2] Multiple Mirror Telescope Observatory, University of Arizona, Tucson, AZ 85721, USA
[3] Sterrewacht Leiden, Postbus 9513, NL-2300 RA Leiden, The Netherlands

Received August 5, 1991; accepted March 24, 1992

Abstract. We report MMT observations at 1 Å spectral resolution of the QSO 0000-263 ($z_{em} = 4.11$) in the Ly-α forest between 4050 Å and 4950 Å. A computer code has been developed for setting the continuum level in the forest and for fitting blends with a minimum number of components. We have identified 221 absorption lines in the observed window and present evidence for high column-density systems at $z_{abs} = 3.3905$ and 3.0533, the latter previously unreported. The $z = 3.39$ system is the highest redshift damped Ly-α system known, having $N(H) = 2 \times 10^{21}$ cm^{-2}. We find no convincing evidence for strong molecular hydrogen absorption in this system. At an adopted excitation temperature of $T_{ex} = 1000K$ and a Doppler width of 25 km s^{-1}, we set an upper limit to the fractional H_2 abundance of $f \leq 3 \times 10^{-6}$ which is lower than a typical Galactic value for high column-density interstellar clouds by a factor of nearly 10^5.

Key words: quasars: individual – intergalactic medium – interstellar medium: molecules

1. Introduction

In a series of papers of which this a member (Chaffee *et al.* 1986, hereafter Paper I; Black *et al.* 1987, hereafter Paper II; Chaffee *et al.* 1988, hereafter Paper III; Foltz *et al.* 1988, hereafter Paper IV; and Levshakov *et al.* 1989, hereafter Paper V), we concentrated our attention on the search for molecular transitions in absorbing clouds toward high redshift QSOs. Molecules should play a vital role in the heat balance of interstellar matter in young galaxies, since they are one of the significant cooling agents of interstellar gas in star-forming regions. They are likely to be detectable only in clouds of high column density, and thus in Papers II-V we searched for them in the so-called "Ly-α disk" systems. These systems are believed to arise in galactic disks (Wolfe 1986) or in gas-rich dwarf galaxies (Pettini *et al.* 1990) along the line-of-sight to background QSOs, and have heavy-element abundances of the order of 10^{-1} to 10^{-2} times the solar value (see Papers II and III).

In Paper II, we searched for H_2 absorption in the well-known Ly-α disk system at $z_{abs} = 2.309$ toward PHL 957 ($z_{em} = 2.681$). By identifying anti-coincidences between the observed spectrum and a synthetic H_2 spectra for a range of excitation temperatures, we were able to set an upper limit on the fraction of hydrogen in molecular form, $f \leq 4 \times 10^{-6}$ ($f = 2N(H_2)/N(H)$, where $N(H_2)$ and $N(H)$ are the total column densities of H_2 and H, respectively). For Galactic interstellar molecular clouds with $N(H) > 10^{19}$ cm^{-2}, the mean value of f is 0.25 (Savage *et al.* 1977), so our inferred upper limit in the $z_{abs} = 2.309$ system is lower than the corresponding Galactic value by a factor of nearly 10^5.

In Papers II, III, and V we further set upper limits of 3×10^{-9} on the value of $N(CO)/N(H)$ in the aforementioned system toward PHL 957 and in the $z_{abs} = 1.776$ system toward MC 1331+170 ($z_{em} = 2.081$). In Galactic diffuse clouds this ratio varies from 3×10^{-6} toward ζ Oph to 2×10^{-9} toward π Sco (Federman *et al.* 1980). Thus the limits on $N(CO)/N(H)$ in the damped Ly-α systems are of the same order as the smallest value reported in a Galactic diffuse interstellar cloud.

Lanzetta *et al.* (1989) also searched for H_2 in the $z_{abs} = 2.796$ damped Ly-α absorber toward 1337+113 ($z_{em} = 2.919$), and were able to set an upper limit $f < 1.3 \times 10^{-4}$, which is lower than typical Galactic values by about three orders of magnitude.

These results combine to suggest that physical conditions in the absorbers toward PHL 957, MC 1331+170 and Q 1337+113 differ significantly from those found in diffuse interstellar clouds at the present epoch. The extremely low inferred value of the molecular fractions in these systems would seem to arise from two possible causes: (1) a higher intensity of UV radiation relative to average gas density at this epoch, and (2) a lower dust-to-gas ratio in the absorbing clouds.

Send offprint requests to: S.A. Levshakov

* Observations reported here were obtained with the Multiple Mirror Telescope, a facility operated jointly by the Smithsonian Institution and the University of Arizona.

** Visiting Astronomer, Space Telescope Science Institute, which is operated by the Association of Universities for Research in Astronomy, Inc. under contract with the National Aeronautics and Space Administration.

*** Senior Visiting Fellow, Institute of Astronomy, Cambridge, UK, 1 July 1990 - 1 August 1991

**** Present address: Steward Observatory, University of Arizona, Tucson, AZ 85721, USA

Slightly apart from these general conclusions are the results of Paper IV in which we present evidence for a positive detection of H_2 absorption in the $z_{abs} = 2.811$ damped Ly-α system toward PKS 0528–250 ($z_{em} = 2.770$). The inferred fractional H_2 abundance of 10^{-3} remains lower than the mean Galactic value by a factor of 4×10^{-3}, although such small molecular fractions are observed in the Galaxy toward slightly reddened stars. In some cases, molecular abundances at this level can be attributed to regions of compressed neutral gas in front of the outward-moving shocks produced by expanding H II regions. More recently Levshakov *et al.* (1991) have presented tentative evidence for the presence of CO in this same $z_{abs} = 2.811$ cloud. They infer an upper limit of 10^{-5} on $N(CO)/N(H_2)$ which is of the same order of magnitude as that found in diffuse Galactic clouds of comparable $N(H_2)$. However, the velocity of this damped Ly-α system is nearly 3200 km s^{-1} higher than that of the background QSO, which would seem to imply a closer association of the absorber with the QSO nucleus than is usually the case. Therefore, the absorbing material may be more severely influenced by the QSO than is typical of other Ly-α disk systems.

In this paper, we consider another "classical" damped Ly-α system whose redshift ($z_{abs} = 3.391$) places it far from its illuminator, Q0000–263 ($z_{em} = 4.11$). This system, first reported by Webb *et al.* (1988), is the Ly-α disk system of highest known redshift, having an age of about 11% of the present age of the Universe ($q_0 = 0.5$). D'Odorico and Savaglio (1991) have recently estimated a metallicity of $Z/Z_\odot < 1/30$ for this system, based on absorption line measurements of Zn II lines.

In what follows we examine evidence for H_2 absorption in this system. Section 2 presents the observational material and data-reduction procedures. Section 3 is concerned with the analysis of the data. The interpretation of the data is addressed in Section 4 and 5, where a brief analysis of a newly discovered absorption-line system is given. The results are then summarized in Section 6.

2. Observations and reductions

Spectroscopic observations of 0000–263 were obtained on the night of 1988 November 11 (UT) using the Multiple Mirror Telescope (MMT) with the blue channel of the MMT spectrograph equipped with a photon-counting intensified Reticon detector. A total integration of 190 minutes was obtained using the 832 g/mm grating blazed at 4000 Å in second order, and the data cover the range 4050Å ≤ λ ≤ 4950Å. To block first-order light a solid $CuSO_4$ filter was used. All observations were made using the "image stacker" (Chaffee and Latham 1982) which produces 1 Å resolution with 2.5 arcsecond circular entrance apertures.

The data were flat-fielded and wavelength-mapped as described in Paper I, and we will not discuss our procedures further here except to note that the spectra were corrected for neither atmospheric extinction nor wavelength-dependent sensitivity of the instrument. All wavelengths and redshifts quoted or displayed in this paper are vacuum, heliocentric values.

Figure 1 presents the resulting spectrum of 0000–263, where the 1σ noise level is plotted at the bottom. The measured signal-to-noise ratio (S/N) is ≃ 12 at λ ≃ 4800Å and ≃ 2 at λ ≃ 4100Å. Such a decrease in S/N at the blue end of the spectrum reflects, in part, the decrease of the absolute blue flux of 0000–263 caused by: (a) the redshifted Lyman continuum edge at λ4660 (marked as L_c in Figure 1) and (b) the high-density Ly-α forest. This characteristic of the 0000–263 continuum is corroborated by the high-S/N, moderate-resolution spectra obtained by Sargent *et al.* (1989) and by Schneider *et al.* (1989) which show a continuum depression beginning shortward of λ6200 with a further break below λ4660.

3. Data analysis

3.1. Continuum level placement

Our measurements of strengths of absorption features in the spectrum of 0000–263 depend critically, of course, on our chosen continuum placement. This placement was made by a computer procedure similar to that described by Young *et al.* (1979).

First, the spectrum was divided into consecutive segments of random length. Following Young *et al.*, we then calculated a series of (λ,μ) pairs where λ is the mean wavelength of the points in a segment and μ is their mean count level. These (λ,μ) pairs were then spline-fitted with cubic polynomials, and this fit was used as the first approximation to the continuum level. Subsequently, a new set of consecutive segments of random length was calculated and the procedure was repeated many times for the calculation of the average continuum level and its variance at each pixel.

The accuracy, $\langle \sigma_c/C \rangle$, per pixel of such continuum level fitting was found to be about 1-2% in the region of low line density, and about 6 - 12% in the high-density Ly-α forest. Since, however, the real data may be perturbed by non-Gaussian fluctuations such as the presence of numerous unresolved weak lines, the inferred continuum may be depressed from the "true" one. The smooth thick curve displayed in Figure 1 is the adopted continuum level, and the thin curves on either side of the continuum denote the $\pm 1\sigma_c$ errors.

3.2. Selection of absorption lines

The normalized spectrum of 0000–263 is shown in Figure A1 in the Appendix. A candidate absorption line was deemed to be real if its equivalent width, W, was greater than thrice the standard deviation, σ_{lim}, of the equivalent width. Following Bohlin *et al.* (1983), the variance in equivalent width measurements is given by:

$$\sigma_W^2 = \left[\sum_{i=1}^{M} \left(\frac{S}{N} \right)_i^{-2} + \left\langle \frac{\sigma_c}{C} \right\rangle^2 (M - W)^2 \right] \Delta\lambda^2, \quad (1)$$

where $(S/N)_i$ is the signal-to-noise ratio in the i*th* pixel; $\langle \sigma_c/C \rangle$ is the mean accuracy of the continuum fit over the width of the line; M is the number of pixels involved in the sum; W is the equivalent width in pixels; and $\Delta\lambda$ is the width of each pixel in Å. We then define the equivalent width detection limit as

$$\sigma_{lim} = \left(\left\langle \frac{S}{N} \right\rangle^{-2} \mathcal{M} + \left\langle \frac{\sigma_c}{C} \right\rangle^2 \mathcal{M}^2 \right)^{1/2} \Delta\lambda. \quad (2)$$

If we assume a width of $\mathcal{M} = 2.5 \times$FWHM to be typical of the full width at the continuum level of an unresolved, unblended weak absorption feature, we can calculate the minimum detectable equivalent width, which we adopt to be $W_{min} = 3\sigma_{lim}$. This limit, which we have used to select the absorption lines or to set

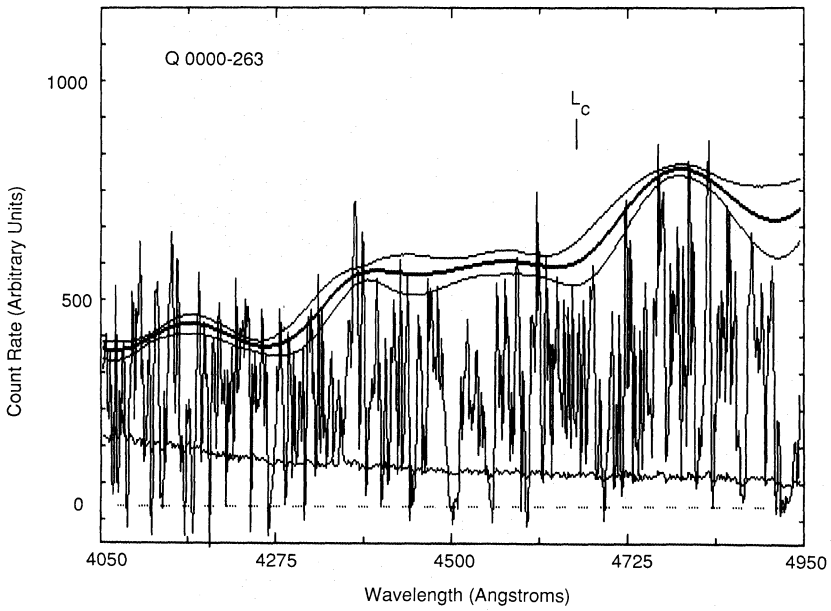

Fig. 1. 1 Å resolution spectrum of Q 0000–263 obtained with the MMT spectrograph. The lower curve presents the 1σ level as derived from counting statistics in the object and night sky spectra (plus dark emission). The zero intensity level is indicated by the horizontal dashed line. The thick solid line represents the average continuum level fitting as described in the text. Two thin lines on either side of this denote $\pm 1\sigma$ errors in such fitting. The position of the Lyman continuum edge in the emission is marked as L_c.

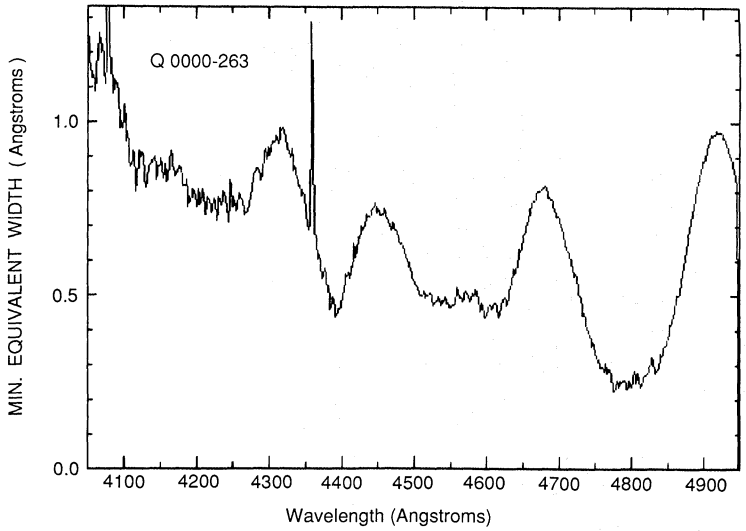

Fig. 2. The 3σ upper limit on the equivalent width, W_{lim}, of an unblended, unresolved absorption line as a function of wavelength.

limits on the strengths of weak lines, is shown as a function of wavelength in Figure 2 .

For weak absorption features ($W \ll 1$), the second term in equation (1) is about the same order of magnitude as the first, meaning that, not surprisingly, the detection of weak absorption lines is very sensitive to the accuracy of the continuum fitting. Moreover, in the case of variations in the S/N and σ_c/C across the spectrum, W_{min} will increase as the data become more noisy.

The list of absorption lines selected in this way is given in the appendix (Table A1). It should be noted that the spectrum of 0000–263 exhibits an extremely high density of absorption lines, most of which are blends even at 1 Å resolution. The ability to resolve blends also depends on S/N, so that some apparently single features may be multiple in our data. In order to calculate the absorption-line parameters listed in Table A1, we have used a standard profile-fitting procedure in which χ^2 is minimized. We have further attempted to fit complex absorption features with a minimum number of components. To illustrate this procedure, we have plotted in Figure 3 the decomposition of blends in the vicinity of the strong $z_{abs} = 3.391$ Ly-β absorption.

The values of τ_0 and b inferred in this way from blended lines are rather uncertain in relatively low resolution data such as we present here, and we have used their values only for the calculation of the equivalent width which is invariant. We have determined σ_W and σ_λ separately for each component of each blend. The equivalent width error follows directly from equation (1), and we have used equation (A15) from Bohlin *et al.* (1983) to calculate the wavelength error:

$$\sigma_\Lambda^2 \approx \left(\frac{\Delta\lambda}{W}\right)^2 \left\langle \frac{S}{N} \right\rangle^{-2} \frac{M^3 \Delta\lambda^2}{12}. \quad (3)$$

The standard error in the wavelength scale calibration, σ_s, is given by the quadratic sum $\sigma_\lambda^2 = \sigma_\Lambda^2 + \sigma_s^2$ (where $\sigma_s = 0.16$ Å in our case). The resulting full line list is given in Table Al, which contains the ordinal number of the line, its central wavelength and associated error, its equivalent width and associated error,

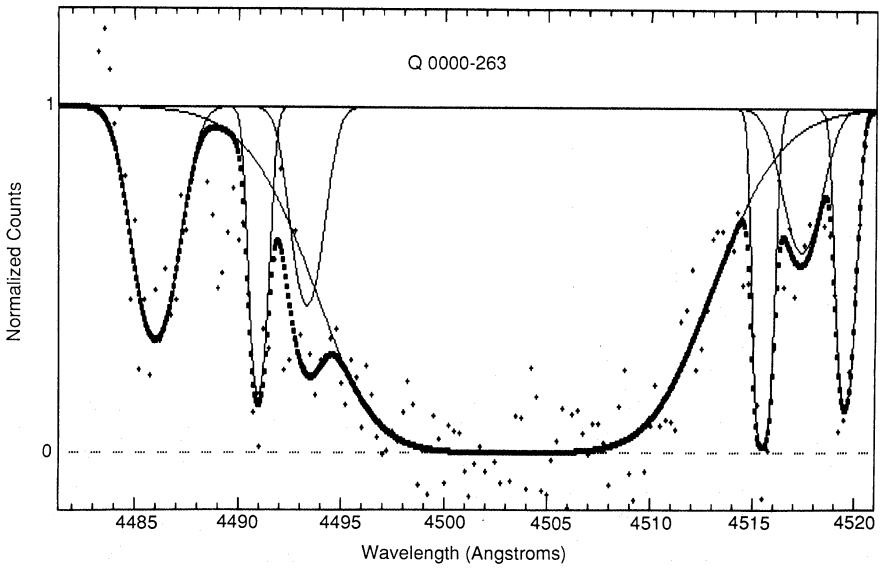

Fig. 3. Portion of the normalized spectrum of Q 0000–263 (crosses), centered on the Lyman–β line at $z_{abs} = 3.391$. Thick line is the computed profile of a blend which has been split into 7 components (thin lines) as described in the text. All 21 adjusting parameters [(τ_0, λ, b) per line] were calculated simultaneously by minimizing both the χ^2 value and the number of components.

and some possible identifications. All absorption lines listed in Table A1 are indicated by tick marks in Figure A1.

4. Atomic and molecular hydrogen in the Cloud at $z_{abs} = 3.391$

4.1. Atomic hydrogen and metal species

As was mentioned in Section 1, our rather narrow observing window is not suitable for detailed analysis of physical conditions in the $z = 3.391$ cloud toward 0000–263. However, the extremely strong Ly-α line seen by others at λ5340 is an example of absorption by a "Ly-α disk", and is similar to that at $z = 2.309$ toward PHL 957 which we analysed in Paper II. Both systems have a neutral hydrogen column density $N(\mathrm{H}) \geq 2 \times 10^{21}$ cm^{-2}, and we will adopt some of the physical parameters inferred for the system toward PHL 957 for the analysis that follows.

Webb *et al.* (1988) have presented 0.5 Å resolution observations of the $z = 3.391$ Ly-α line toward 0000–263. From their Voigt profile fit of the line, they infer a value of $N(\mathrm{H}) = 3 \times 10^{21}$ cm^{-2}. Sargent, Steidel and Boksenberg (1989) also report observations of this line at 6 Å resolution and very high S/N which they have used to infer a value of $N(\mathrm{H}) = 2 \times 10^{21}$ cm^{-2}. These authors also detected absorption by Si II and C IV from this system. Steidel (1990) has identified C II and O I, as well. Finally, D'Odorico and Savaglio (1991) report $N(\mathrm{H}) = 2.5 \times 10^{21}$ cm^{-2}.

Many of the higher order Lyman lines in this system are in our observed spectral window shown in Figures 1 and A1. Unfortunately, however, only Ly-β could be used for quantitative analysis, since Ly-γ at λ4270 is an unresolved blend and the S/N becomes extremely low shortward of that wavelength. We have thus made no attempt to analyse any of the higher-order Lyman lines.

Given a neutral hydrogen column density in the range $(2-3) \times 10^{21}$ cm^{-2}, the Ly-α and Ly-β lines should lie on the square root portion of the curve of growth where their equivalent widths are given by:

$$W_\lambda = \frac{2\pi e^2 \lambda f}{m_e c^2} \left(\frac{2g_1}{g_2} N \right)^{1/2}, \qquad (4)$$

(Spitzer 1978). Thus the corresponding column density is:

$$N(\mathrm{H}) = 7.27 \times 10^{19} \left[\frac{W_{obs}(L_\beta)}{1 + z_{abs}} \right]^2 \quad (\mathrm{cm}^{-2}), \qquad (5)$$

where $W_{obs}(L_\beta)$ is the observed value of the Ly-β equivalent width in Å. Substituting our observed value of 19.9 ± 3.5 Å (3σ) for $W_{obs}(L_\beta)$, we find $N(\mathrm{H}) = (1.5 \pm 0.5) \times 10^{21}$ cm^{-2} for the absorbing cloud at $z = 3.391$. This value is in satisfactory agreement with the H I value found by Sargent *et al.* (1989), but somewhat below that of Webb *et al.* (1988). If the former is correct then the consistency between the value we infer from Ly-β would suggest that our continuum location and the deconvolution procedure in its vicinity are reasonably accurate. However, the higher Webb *et al.* $N(\mathrm{H})$ value provides a cautionary note in this regard.

It should be noted that C III λ977 is, presumably, present in the $z = 3.391$ absorption system. It is a resolved component of a blend at λ4288, and its rest equivalent width is 0.6 ± 0.3 Å (3σ). Chaffee *et al.* (1986) pointed out that C III λ977 is expected to be the strongest observable metal line in QSO absorption systems over a wide range of $N(\mathrm{H})$. Some care must be taken in inferring C^{++} column densities from this line in our data, however, because it lies in a region of high line density and because the appropriate Doppler parameter is not known.

4.2. Molecular hydrogen

We now turn our attention to the search for molecular hydrogen absorption in the dense Ly-α forest of 0000–263. The high line density dictates the need for as precise an estimate as possible of the absorption redshift of the system, and we adopt the mean value of $z_{abs} = 3.39051 \pm 0.00007$ inferred from C III λ977 and the neutral hydrogen lines listed in Table A1.

We adopt the rest wavelengths and oscillator strengths of H_2 lines corresponding to transitions of the Lyman $B\,^1\Sigma_u^+ \leftarrow X\,^1\Sigma_g^+$ and Werner $C\,^1\Pi_u^\pm \leftarrow X\,^1\Sigma_g^+$ bands published by Morton and Dinerstein (1976). In the rest frame, some of them are coincident with absorption lines listed in Table A1, but a large number are blended with strong Ly-α forest lines at different redshifts.

The inferred H_2 column density depends on the excitation temperature, T_{ex}, and the Doppler parameter, b. Typical diffuse

molecular clouds in the Galaxy have a mean $J = 0/J = 1$ excitation temperature of $\langle T_{01} \rangle = (77 \pm 17)$ K, with the bulk lying in the range between 45 and 128 K (Savage *et al.* 1977). For the more tenuous diffuse clouds, T_{ex} can be as high as 1000 K for $J = 0-5$ (Morton and Dinerstein 1976). Furthermore the interstellar molecular clouds of moderate and high fractional H_2 abundance, $f > 0.05$, exhibit a tendency toward low excitation temperature $T_{ex} \sim 100$ K (Spitzer and Jenkins 1975), and molecular clouds with $f < 0.05$ tend to higher T_{ex}. The behavior of the Doppler parameter in these various conditions is uncertain.

In Paper II, a curve-of-growth analysis of the metal lines of the $z_{abs} = 2.309$ damped Ly-α system toward PHL 957 yielded a value of $b = 25\,\mathrm{km\,s^{-1}}$, and we adopt this value as a fairly conservative upper limit in the analysis that follows.

To obtain quantitative estimates of $N(H_2)$ and T_{ex}, we choose small continuum "windows" where some H_2 transitions are expected but no absorption features were observed. The most stringent limit is set by the absence of the L(4-0)R(1) transition at λ4609.85 for which the 3σ upper limit was $W_{rest} < 114$ mÅ. In addition, line Number 67 with $W_{rest} = 182$ mÅ lies near the predicted position of W(0-0)R(0)+R(1), and we adopt 182 mÅ as the upper limit of its strength.

The strongest *UV* absorption lines of H_2 arise from the first rotational levels, and the relative population of these states is determined by the excitation temperature of the gas. In thermal equilibrium, the ratio of column densities is given by:

$$\frac{N(J)}{N(0)} = \frac{g_J}{g_0} \exp\left[-\frac{BJ(J+1)}{kT_{ex}}\right], \tag{6}$$

where the statistical weight of a level J in the ground state $X\,^1\Sigma_g^+$ is $3(2J+1)$ for odd J and $(2J+1)$ for even J, and the constant $B/k \approx 85$ K.

Following Spitzer (1978) the equivalent width of an interstellar absorption line is determined by:

$$\frac{W}{\lambda} = \frac{2b}{c} F(\tau_0), \tag{7}$$

$$F(\tau_0) = \int_0^\infty \left[1 - \exp\left(-\tau_0 e^{-x^2}\right)\right] dx, \tag{8}$$

and the central optical depth, τ_0, is given by

$$\tau_0 = \frac{1.497 \times 10^{-10}}{b} N\lambda f, \tag{9}$$

where f is the oscillator strength of the transition, λ its rest wavelength, W its rest equivalent width (both in Å) and b is the Doppler parameter in cm s^{-1}.

Using the above-mentioned limits on $W_{L(4-0)} < 114$ mÅ and $W_{W(0-0)} < 182$ mÅ and equations 6-9 the following inequalities are easily derived:

$$N(0) < 1.1 \times 10^{14} \exp(170/T_{ex}), \tag{10}$$

based on the equivalent width limit of the L(4-0)R(1) line and

$$N(0) < \frac{2 \times 10^{14}}{0.2 + \exp(-170/T_{ex})}, \tag{11}$$

based on the $W_{W(0-0)}$ limit.

The locus of possible values of $N(0)$ and T_{ex} is shown in Figure 4, where it can be seen that $N(0)$ lies in the range from $6.3 \times 10^{14}\,\mathrm{cm^{-2}}$ at $T_{ex} = 77$ K to $1.3 \times 10^{14}\,\mathrm{cm^{-2}}$ at $T_{ex} = 1000$ K.

Taking into account that at low molecular fraction the excitation temperature might be as high as 1000 K, the upper limit to the $N(0)$ column density should be closer to $1.3 \times 10^{14}\,\mathrm{cm^{-2}}$. From this we infer a total H_2 column density of $N(H_2) = \sum_J N(J) < 3.1 \times 10^{15}\,\mathrm{cm^{-2}}$. This value implies an upper limit to the fractional H_2 abundance of $f < 3 \times 10^{-6}$. Thus, the inferred value of the molecular fraction in the cloud toward 0000–263 is similar to that of $f < 4 \times 10^{-6}$ reported in Paper II in the damped Ly-α system toward PHL 957.

It should be noted that what we observe is an upper limit to the equivalent width of any line, and the equivalent width is a function of N/b. Equivalent-width-limited observations cannot break this N, b degeneracy, and our inferred molecular fraction upper limit is strongly dependent on the assumed value of b. If, for example, b is $5\,\mathrm{km\,s^{-1}}$ instead of $25\,\mathrm{km\,s^{-1}}$ as we have adopted, the upper limit to the value of $N(0)$ would increase two hundred-fold, with a concomitant increase in the inferred upper limit to the molecular fraction. Only the *positive detection* of molecular lines at high resolution and high S/N will remove this degeneracy.

As for providing a more stringent observational constraint on the value of the excitation temperature, at $T_{ex} \sim 1000$ K, rotational levels $J = 0-5$ of H_2 will all be significantly populated, and the large number of possible lines arising in them will create a "molecular hydrogen forest". In our case the strongest Werner lines in this forest would have equivalent widths which could be observable at our detection limit were the line blending not so severe.

5. A possible Lyman-Limit System at $z_{abs} = 3.053$

As a by-product of our analysis we have tentatively identified an additional absorption-line system toward 0000–263 with $z_{abs} = 3.0533 \pm 0.0002$. This system is identified on the basis of only three absorption lines: Ly-α, Ly-β and Si III. The identity of Ly-β is somewhat suspect since it lies in the noisy portion of our spectrum. Among the metal lines, only Si III λ1206 may be identified unequivocally in our spectral region. The rest equivalent width of the rather strong Ly-α line is $W_0 = 4.6 \pm 0.4$ Å, which yields an H I column density $\sim (4.3 \pm 0.7) \times 10^{19}\,\mathrm{cm^{-2}}$ at any reasonable Doppler parameter ($b < 200\,\mathrm{km\,s^{-1}}$). If this identification is correct, the H I column density places this absorbing cloud among the population of the so-called "Lyman-Limit Systems" (LLS) which Sargent, Steidel and Boksenberg (1989) have postulated as associated with distant galaxies. Our finding at least two LLS with $z > 3$ toward 0000–263 is in good agreement with the observed distribution of the number density of LLS per unit redshift range:

$$\frac{dN}{dz} = 0.76 \times (1+z)^{0.68 \pm 0.54}, \tag{12}$$

inferred by Sargent, Steidel and Boksenberg.

6. Summary: Current status of molecules at early epochs

Our latest upper limit on the H_2 column density at $z = 3.391$ adds to a growing list of such upper limits. Table 1 summarises

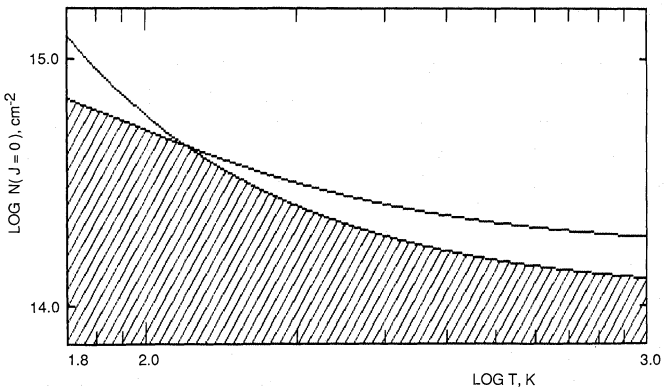

Fig. 4. Shaded area is a range of possible values of the H_2 column density at the lowest level $J = 0$ of the ground state $\left(X^1\Sigma_g^+\right)$ and the excitation temperature based on inequalities (10) and (11). The point, representing the upper limits of 1.3×10^{14} cm^{-2} on the $N(H_2, J = 0)$ and of 1000 K on the T_{ex}, is the top right hand corner of the shaded area.

Table 1. Molecules in damped Ly-α systems at early epochs

QSO :	0000-263	0100+130	0528-250	1331+170	1337+113
z_{em}	4.110	2.681	2.770	2.081	2.919
z_{abs}	3.391	2.309	2.811	1.776	2.796
$N(HI)$, cm^{-2}	2×10^{21}	2.5×10^{21}	2×10^{21}	1.5×10^{21}	8×10^{20}
$N(H_2)$, cm^{-2}	$< 3 \times 10^{15}$	$< 5 \times 10^{15}$	$\approx 10^{18}$	...	$< 5 \times 10^{16}$
$N(CO)$, cm^{-2}	...	$< 7 \times 10^{12}$	$< 1.3 \times 10^{13}$	$< 4 \times 10^{12}$	...
f_{H_2}	$< 3 \times 10^{-6}$	$< 4 \times 10^{-6}$	$\approx 10^{-3}$	...	$< 1.3 \times 10^{-4}$
f_{CO}	...	$< 3 \times 10^{-9}$	$< 6.5 \times 10^{-9}$	$< 3 \times 10^{-9}$	...
Ref	a	b,c	d,e	f,c	g

REFERENCES: a - this work; b - paper II; c - paper V; d - paper IV; e - Levshakov *et al.* (1991); f - paper III; g - Lanzetta *et al.* (1989)

NOTE: f_{H_2},f_{CO} are the fractional H_2 and CO abundances.

the upper limits and detections of molecular absorption at $z > 2.0$ to date.

It is quite striking that the only significant evidence for a detection of H_2 occurs in an absorbing cloud whose redshift exceeds that of the illuminating QSO. Such a cloud is presumably associated with the QSO host galaxy and would experience dramatically different physical conditions from those in more typical "intervening" absorbing clouds. It would be of great interest to identify more examples of high column density "associated" clouds in which to search for molecular absorption.

It would also be interesting to investigate in more detail the metallicities and ionization parameters in systems with low values of f. One possible explanation of the absence of H_2 is simply that the abundance of dust particles (expected to be related to average metallicity) is too low for efficient formation of H_2 by surface catalysis. Another testable explanation (cf. Paper II, for example) is that the ratio of UV photon density to mean gas density is high enough to favor free atoms in the H/H_2 balance, even when the total column density of hydrogen exceeds 10^{21} cm^{-2}. If indeed the damped Ly-α systems arise in large disk galaxies, then the interpretation of the absorption lines would be greatly enhanced by measurements of emission lines from H I and CO in the same regions.

Acknowledgements. S.A.L. thanks his colleagues at the STScI for their hospitality and assistance in utilizing the facilities of the Institute and for the support of a Guest Research Fellowship at the STScI. F.H.C. gratefully acknowledges the hospitality of the Institute of Astronomy and the support of a Royal Society Guest Research Fellowship; he further wishes to acknowledge the hospitality of the Ioffe Institute during his visit in September 1990. C.B.F. acknowledges support of the National Science Foundation via NSF 90-01181. J.H.B. is grateful to Leiden Observatory for hospitality and facilities.

Appendix A: Spectral data and line list for Q 0000-263

Table A1. Absorption line list for Q0000–263

No.	λ (Å)	σ_λ (Å)	W_{obs} (Å)	σ_W (Å)	*ID*	z_{abs}
1	4060.50	0.22	1.37	0.42		
2	4065.25	0.21	1.65	0.46		
3	4066.89	0.23	1.32	0.41	H I λ926	3.39080
4	4068.13	0.23	1.40	0.43		
5	4073.34	0.28	3.66	0.72		
6	4084.60	0.21	1.58	0.47		
7	4086.30	0.20	1.93	0.52	H I λ931	3.39033
8	4107.50	0.32	2.27	0.47		
9	4110.75	0.36	1.95	0.44		
10	4115.70	0.20	1.47	0.38		
11	4117.48	0.19	2.37	0.48	H I λ938	3.3906
12	4129.97	0.23	6.14	0.78		
13	4135.66	0.34	2.03	0.45		
14	4146.82	0.22	1.44	0.37		
15	4154.01	0.21	2.69	0.51		
16	4157.15	0.23	2.22	0.47	H I λ1026	3.0529
17	4159.69	0.21	2.36	0.48		
18	4164.23	0.26	1.51	0.38		
19	4168.01	0.19	1.62	0.40		
20	4169.74	0.22	2.09	0.45	H I λ950	3.3904
21	4170.85	0.21	3.14	0.56		
22	4181.25	0.25	2.79	0.52		
23	4191.52	0.21	3.55	0.56		
24	4200.00	0.26	1.67	0.38		
25	4208.03	0.31	1.31	0.34		
26	4212.61	0.21	2.45	0.46		
27	4216.84	0.34	1.71	0.38		
28	4222.13	0.23	2.04	0.42		
29	4227.45	0.31	1.04	0.30		
30	4244.40	0.19	2.58	0.47		
31	4250.95	0.25	0.85	0.27		
32	4267.35	0.21	4.38	0.62		
33	4271.15	0.21	3.24	0.53		
34	4275.19	0.39	2.46	0.46		
35	4287.27	0.25	3.45	0.58		
36	4289.71	0.23	2.56	0.50	C III λ977	3.3906
37	4296.87	0.21	1.73	0.41		
38	4301.37	0.20	2.47	0.49		
39	4303.64	0.22	1.39	0.37		
40	4308.99	0.24	1.36	0.36		
41	4313.39	0.19	3.43	0.61		
42	4323.94	0.26	1.21	0.36		
43	4327.56	0.21	2.82	0.50		
44	4332.53	0.18	1.19	0.32		
45	4334.00	0.18	1.23	0.33		
46	4337.87	0.21	1.60	0.37		
47	4340.52	0.19	1.90	0.41		
48	4342.55	0.26	1.64	0.38		
49	4345.32	0.19	1.11	0.31		
50	4350.12	0.25	2.64	0.48		
51	4352.89	0.25	1.91	0.41		
52	4355.91	0.27	1.30	0.33		
53	4361.97	0.30	2.11	0.43		
54	4364.39	0.18	1.23	0.33		
55	4366.72	0.29	1.00	0.29		
56	4383.32	0.21	2.17	0.38		
57	4392.28	0.19	3.70	0.45		
58	4395.43	0.22	1.24	0.26		
59	4397.55	0.21	1.19	0.25		
60	4399.62	0.19	0.73	0.20		
61	4401.02	0.20	0.92	0.22		
62	4402.20	0.19	0.67	0.19		
63	4407.54	0.18	1.14	0.25		
64	4412.61	0.20	5.78	0.56		
65	4420.33	0.18	4.68	0.55		
66	4424.85	0.32	1.09	0.26		
67	4428.39	0.27	0.78	0.22		
68	4432.06	0.19	3.24	0.50		
69	4438.33	0.19	3.15	0.49		
70	4441.80	0.22	1.01	0.28		
71	4448.30	0.19	3.81	0.58		
72	4453.23	0.19	7.17	0.79		
73	4460.81	0.24	0.83	0.27		
74	4464.50	0.19	2.72	0.45		
75	4468.20	0.18	3.11	0.49		
76	4478.52	0.25	1.15	0.29		
77	4481.47	0.30	1.34	0.32		
78	4485.99	0.23	1.82	0.37		
79	4490.95	0.18	0.93	0.26		
80	4493.29	0.23	1.15	0.27		
81	4503.32	0.23	19.85	1.15	H I λ1026	3.3904
82	4515.45	0.17	1.16	0.25		
83	4517.34	0.32	0.99	0.23		
84	4519.51	0.17	1.02	0.23		
85	4523.69	0.20	1.47	0.28		
86	4525.82	0.21	1.13	0.25		
87	4527.64	0.19	1.52	0.29		
88	4530.00	0.24	1.45	0.28		
89	4531.73	0.21	0.97	0.23		
90	4535.35	0.20	1.08	0.24		
91	4536.88	0.17	1.79	0.31		
92	4538.83	0.21	0.76	0.20		
93	4541.38	0.20	2.51	0.37		
94	4544.39	0.17	1.88	0.32		
95	4545.95	0.17	1.18	0.25		
96	4551.55	0.19	9.75	0.73		
97	4556.24	0.19	1.33	0.27		
98	4561.89	0.17	1.17	0.25		
99	4563.65	0.26	0.76	0.20		
100	4565.62	0.17	1.01	0.23		
101	4567.09	0.19	1.41	0.27		
102	4570.51	0.51	0.72	0.20		
103	4572.31	0.21	0.59	0.18		
104	4575.90	0.18	2.38	0.36		
105	4577.54	0.17	0.93	0.22		
106	4579.95	0.18	1.81	0.31		
107	4582.32	0.18	0.87	0.21		
108	4590.56	0.17	2.91	0.40		
109	4593.55	0.19	0.79	0.20		
110	4597.59	0.17	6.20	0.58		

Table A1. (continued)

No.	λ (Å)	σ_λ (Å)	W_{obs} (Å)	σ_W (Å)	*ID*	z_{abs}
111	4601.54	0.18	0.85	0.21		
112	4605.66	0.30	0.67	0.19		
113	4607.58	0.18	0.89	0.22		
114	4614.87	0.18	0.66	0.19		
115	4616.13	0.18	0.88	0.22		
116	4617.70	0.17	1.08	0.24		
117	4618.07	0.18	3.09	0.41		
118	4624.00	0.17	0.81	0.21		
119	4626.70	0.17	1.03	0.23		
120	4627.90	0.19	0.54	0.17		
121	4629.46	0.17	2.11	0.34		
122	4632.80	0.22	0.82	0.21		
123	4635.18	0.21	0.75	0.20		
124	4638.69	0.17	1.24	0.26		
125	4641.31	0.24	1.78	0.31		
126	4643.19	0.18	1.14	0.27		
127	4646.41	0.18	1.35	0.30		
128	4648.35	0.18	1.51	0.31		
129	4652.21	0.17	1.05	0.26		
130	4653.65	0.17	1.51	0.31		
131	4657.23	0.17	1.13	0.29		
132	4659.23	0.17	1.12	0.29		
133	4661.05	0.18	1.65	0.35		
134	4665.82	0.17	1.79	0.37		
135	4667.69	0.19	1.11	0.29		
136	4672.98	0.18	2.49	0.47		
137	4675.92	0.23	1.40	0.35		
138	4684.87	0.18	1.61	0.37		
139	4686.76	0.17	2.55	0.47		
140	4689.17	0.17	2.02	0.42		
141	4691.91	0.16	1.41	0.35		
142	4693.39	0.16	1.22	0.32		
143	4695.88	0.17	3.80	0.58		
144	4698.88	0.17	2.66	0.48		
145	4701.01	0.17	1.15	0.31		
146	4702.36	0.19	1.03	0.28		
147	4704.22	0.18	1.18	0.30		
148	4708.37	0.16	2.26	0.41		
149	4710.56	0.16	2.10	0.40		
150	4713.55	0.17	2.39	0.43		
151	4716.81	0.16	1.30	0.29		
152	4718.33	0.16	1.73	0.33		
153	4720.19	0.17	2.14	0.37		
154	4726.65	0.19	1.92	0.35		
155	4728.72	0.18	0.78	0.22		
156	4732.83	0.17	2.58	0.37		
157	4737.26	0.17	3.26	0.42		
158	4740.07	0.16	1.98	0.33		
159	4742.36	0.23	0.78	0.20		
160	4745.09	0.17	3.50	0.44		
161	4750.23	0.18	1.85	0.28		
162	4752.37	0.17	1.24	0.23		
163	4753.62	0.18	0.93	0.20		
164	4755.17	0.18	1.55	0.26		
165	4757.10	0.16	1.53	0.26		

Table A1. (continued)

No.	λ (Å)	σ_λ (Å)	W_{obs} (Å)	σ_W (Å)	*ID*	z_{abs}
166	4758.56	0.17	1.17	0.22		
167	4761.96	0.16	1.73	0.24		
168	4766.03	0.21	0.43	0.11		
169	4775.16	0.17	3.62	0.34		
170	4777.38	0.17	0.80	0.16		
171	4778.60	0.16	1.22	0.20		
172	4780.69	0.18	0.47	0.12		
173	4781.88	0.17	0.68	0.15		
174	4783.12	0.16	1.11	0.19		
175	4786.05	0.17	0.71	0.15		
176	4787.61	0.17	0.81	0.16		
177	4790.51	0.19	0.98	0.18		
178	4794.00	0.16	3.22	0.32		
179	4798.42	0.17	1.53	0.22		
180	4801.14	0.16	2.18	0.26		
181	4806.70	0.17	1.15	0.19		
182	4807.96	0.18	0.46	0.12		
183	4811.24	0.17	1.25	0.20		
184	4814.12	0.17	5.39	0.42		
185	4817.89	0.16	1.38	0.21		
186	4819.46	0.17	2.06	0.26		
187	4821.49	0.16	1.23	0.20		
188	4823.23	0.18	1.30	0.20		
189	4824.75	0.19	0.46	0.12		
190	4832.33	0.16	1.62	0.23		
191	4834.69	0.16	3.48	0.34		
192	4837.59	0.17	1.46	0.22		
193	4839.35	0.17	1.38	0.21		
194	4843.15	0.17	1.69	0.23		
195	4845.14	0.18	0.54	0.13		
196	4847.63	0.17	1.01	0.18		
197	4850.32	0.17	1.70	0.23		
198	4854.66	0.19	0.81	0.18		
199	4858.33	0.17	1.77	0.28		
200	4861.03	0.17	0.85	0.19		
201	4864.89	0.17	2.44	0.32		
202	4867.44	0.17	1.99	0.33		
203	4871.32	0.16	5.14	0.53		
204	4874.46	0.16	2.89	0.40		
205	4876.60	0.16	1.80	0.31		
206	4878.22	0.17	0.66	0.19		
207	4881.26	0.24	0.97	0.23		
208	4888.50	0.21	1.33	0.32		
209	4890.50	0.18	0.85	0.25	Si III λ1206	3.0535
210	4893.78	0.17	1.92	0.38		
211	4897.76	0.28	1.06	0.32		
212	4901.96	0.17	3.53	0.59		
213	4906.47	0.24	1.34	0.36		
214	4915.05	0.17	4.87	0.73		
215	4927.91	0.17	18.75	1.44	H I λ1216	3.0536
216	4937.67	0.17	1.70	0.43		
217	4940.10	0.17	2.64	0.54		
218	4942.66	0.16	2.66	0.51		
219	4944.77	0.17	1.18	0.34		
220	4946.49	0.17	1.06	0.32		
221	4948.76	0.16	1.93	0.43		

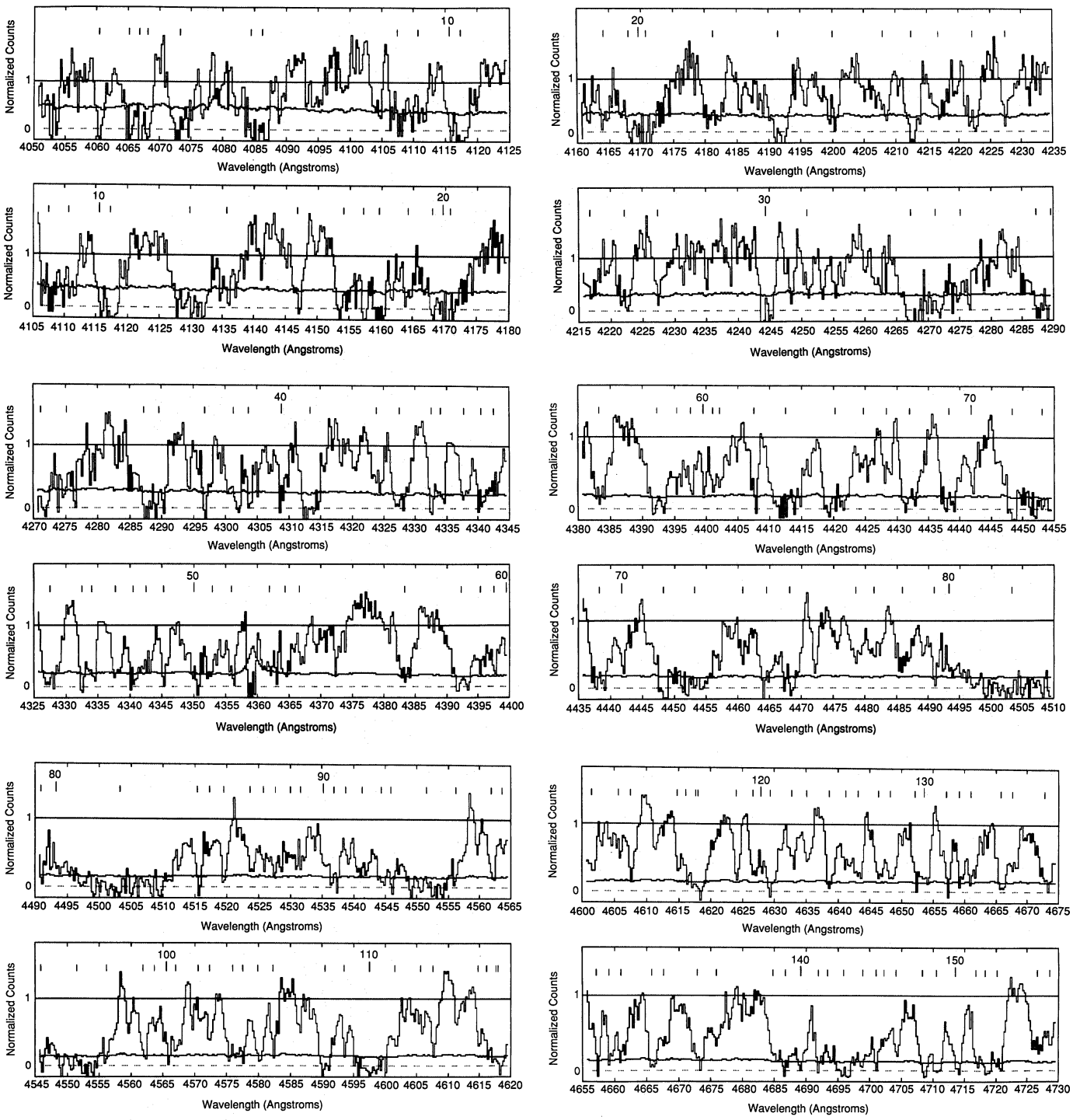

Fig. A1. 1 Å resolution spectrum of Q 0000–263 obtained with the MMT spectrograph. The spectrum has been rectified by the continuum shown in Figure 1 of the main body of the paper. This rectified continuum is marked by a horizontal line at unity and the zero intensity level by a dashed line. The curve between them presents the 1σ level as derived from counting statistics in the object and night sky (plus dark emission) spectra.

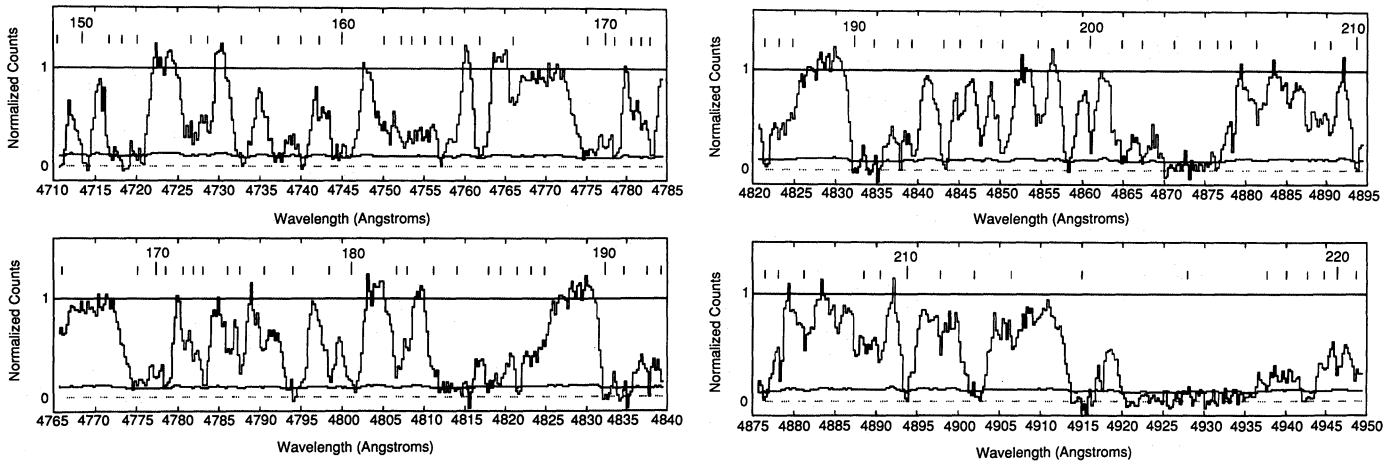

Fig. A1. (continued)

References

Black, J.H., Chaffee, F.H., Foltz, C.B., 1987, ApJ, 317, 442 (Paper II)

Bohlin, R.C., Hill, J.K., Jenkins, E.B., Savage, B.D., Snow, T.P.Jr., Spitzer, L.Jr., York, D.G., 1983, ApJS, 51, 277

Chaffee, F.H.,Jr., Latham, D.W., 1982, PASP, 94, 386

Chaffee, F.H., Foltz, C.B., Black, J.H., 1986, Soviet Astr. Lett., 12, 343 (Paper I)

Chaffee, F.H., Foltz, C.B., Bechtold, J., Weymann, R.J., 1986, ApJ, 301, 116

Chaffee, F.H., Black, J.H., Foltz, C.B., 1988, ApJ, 335, 584 (Paper III)

D'Odorico, S., Savaglio, S., 1991, ESO Sci. Rep. No. 9, p. 51

Federman, S.R., Glassgold, A.E., Jenkins, E.B., Shaya, E.J., 1980, ApJ, 242, 545

Foltz, C.B., Chaffee, F.H., Black, J.H., 1988, ApJ, 324, 267 (Paper IV)

Lanzetta, K.M., Wolfe, A.M., Turnshek, D.A., 1989, ApJ, 344, 277

Levshakov, S.A., Foltz, C.B., Chaffee, F.H., Black, J.H., 1989, AJ, 98, 2052 (Paper V)

Levshakov, S.A., Sargent, W.L.W., Boksenberg, A., Steidel, C.C., 1991, ApJ, submitted

Morton, D.C., Dinerstein, H.L., 1976, ApJ, 204, 1

Pettini, M., Boksenberg, A., Hunstead, R.W., 1990, ApJ, 348, 48

Sargent, W.L.W., Steidel, C.C., Boksenberg, A., 1989, ApJS, 69, 703

Savage, B.D., Bohlin, R.C., Drake, J.F., Budich, W., 1977, ApJ, 216, 291

Schneider, D.P., Schmidt, M., Gunn, J.E., 1989, AJ, 98, 1507

Spitzer, L.,Jr., 1978, Physical Processes in the Interstellar Medium, NY:Wiley-Interscience

Spitzer, L.,Jr., Jenkins, E.B., 1975, Ann. Rev. Astron. Ap., 13, 133

Steidel, C., 1990, ApJS, 72, 1

Webb, J.K., Parnell, H.C., Carswell, R.F., McMahon, R.G., Irwin, M.J., Hazard, C., Ferlet, R., Vidal-Madjar, A., 1988, ESO Messenger, 51, 15

Wolfe, A.M., 1986, Phil. Trans. Roy. Soc. (London), A320, 503

Young, P.J., Sargent, W.L.W., Boksenberg, A., Carswell, R.F., Whelan, J.A.J., 1979, ApJ, 229, 891

This article was processed by the author using Springer-Verlag TEX A&A macro package 1991.